2021 43rd Annual International Conference of the
IEEE Engineering in Medicine & Biology Society (EMBC)
Oct 31 - Nov 4, 2021. Virtual Conference

Development of a non-invasive, dual-sensor handheld imager for intraoperative preservation of parathyroid glands

Eugene Oh, Yoseph Kim, Bo Ning, Seung Yup Lee, Wan Wook Kim and Jaepyeong Cha

***Abstract*— Intraoperative localization and preservation of parathyroid glands (PTGs) are challenging during thyroid surgery. Using a technique of combined near-infrared PTG autofluorescence detection and dye-free imaging angiography, this study developed a portable device for localization of PTGs and assessment of viability by confirming tissue perfusion. The imager's performance was evaluated through a pilot clinical study (N=10).**

***Clinical Relevance*— Postoperative hypocalcemia is a major hypoparathyroidism complication after thyroidectomy. Direct damage to or accidental removal of the parathyroid glands (PTGs) during surgery is one of the main causes of these adverse outcomes. This study aims to develop and translate a portable, noninvasive, and label-free intraoperative imaging tool to aid surgeons to safely localize the PTGs and assess their vascularization.**

I. Introduction

Postoperative hypocalcemia is a major hypoparathyroidism complication after thyroidectomy [1]. In the US, approximately 20 million people are diagnosed with thyroid diseases annually and 150,000 thyroidectomies are performed. Reportedly, 27% of these patients suffer from transient or permanent hypocalcemia, which can lead to lifelong deleterious consequences and impose serious economic burden on patients [2]. Intraoperative preservation of the parathyroid glands (PTGs) can be challenging not only due to their small size and similar appearance to surrounding tissues, but also because the function of normal postoperative PTGs cannot be guaranteed even when they appear to be well-preserved, requiring careful postoperative measurements of calcium and parathyroid hormone (PTH) levels.

The current gold standard is the surgeon's visual identification of PTGs, but the outcomes of this method are inconsistent depending on a surgeon's level of experience and volume of surgeries performed [3]. The PTG tissue is ultimately confirmed by invasive methods such as frozen section analysis and indirectly by intraoperative PTH assays, which require repeated sampling and add 20 - 30 minutes to the operation time per sample. As a non-invasive means, Paras et al. introduced an optical method for identifying PTGs using near-infrared autofluorescence (NIRAF) in 2011 [4]. Although this method was reported to be effective for real-time localization of PTGs [5], it limits the surgeon's ability to evaluate the PTG's viability as the autofluorescence signals are emitted by both viable and non-viable PTGs [6].

In clinical practice, the surgeon's viability assessment can be subjective because they rely on the color change or swelling of the PTGs during visual inspection. A common approach is to look for bright red bleeding after pricking the PTG with a needle but there is a high risk of accidental damage to the healthy glands. Moreover, topical application of a diluted lidocaine solution can cause vasodilation in vascularized PTGs, but this procedure is risky as lidocaine can cause paralysis of the vocal cords if it touches the exposed laryngeal nerves.

Alternatively, recent studies have reported the use of exogenous dyes such as indocyanine green (ICG) for identifying and assessing PTG perfusion, ultimately predicting postoperative hypoparathyroidism [7-9]. However, there are several limitations: it is difficult to capture real-time perfusion information from PTGs due to the delayed onset of ICG fluorescence signals in PTGs; and as the fluorescence signal fades within a few minutes, only one PTG can be observed at a time for perfusion assessment [7]. Moreover, multiple injections of an exogenous dye can possibly lead to adverse allergic reactions in patients [9].

Recently, new surgical devices with non-invasive, dye-free imaging techniques such as laser speckle contrast imaging (LSCI) or hyperspectral imaging (HSI) are being tested intraoperatively to study the vascularity of PTGs; however, these devices are limited by their post-hoc quantitative image analysis. Currently, no practical equipment is capable of real-time display of the PTG perfusion level that can be readily accessible for surgeons to conveniently locate and assess PTGs intraoperatively. In this study, we present a compact, practical solution using a portable imaging angiography technique combined with autofluorescence imaging. Our proposed imaging technique permits seamless real-time visualization of vasculature perfusion and tissue viability assessment for the first time during thyroid procedures.

* Research supported by the National Institute of Biomedical Imaging and Bioengineering of the National Institutes of Health under Award Number R43EB030874 and InTheSmart USA.

E. Oh and Y. Kim are with the Department of Biomedical Engineering, Johns Hopkins University, Baltimore, MD 21218 USA (e-mails: eoh17@jhu.edu and ykim188@jhu.edu).

B. Ning is with the Sheikh Zayed Surgical Institute, Children's National Hospital, Washington DC, 20010 USA (e-mail: bning@cnmc.org).

S. Y. Lee is with the Wallace H. Coulter Department of Biomedical Engineering, Georgia Institute of Technology/Emory University, Atlanta, GA 30322 USA. (e-mail: seung.yup.lee@emory.edu).

W.W. Kim is with the Department of Surgery, Kyungpook National University School of Medicine, Daegu 41404 South Korea. (e-mail: kww1324@naver.com).

J. Cha was with Optosurgical, LLC, Laurel, MD 20723 USA. He is now with the Sheikh Zayed Institute for Pediatric Surgical Innovation, Children's National Hospital, Washington DC, 20010 USA (corresponding author: +1-202-476-6426; fax: +1-202-476-1280; e-mail: jcha2@childrensnational.org).

II. Materials and Methods

A. Device Design and Software Architecture

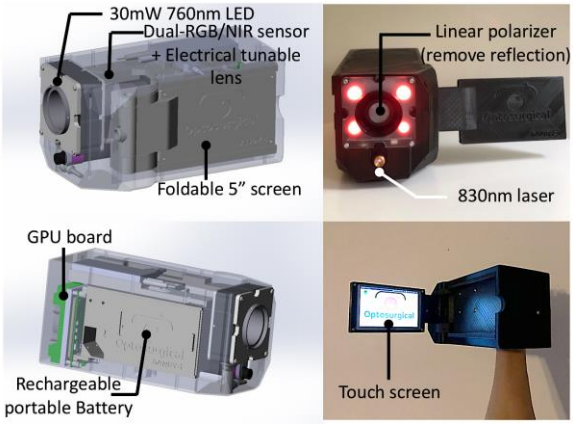

(a)

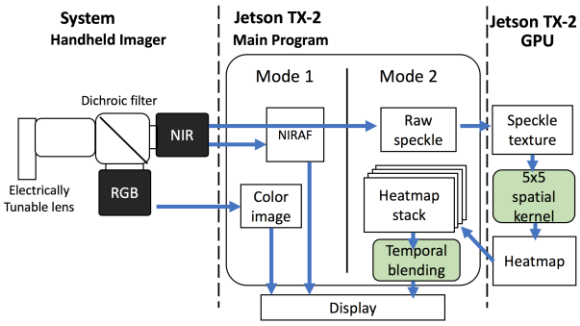

(b)

Figure 1. (a) Components of the portable handheld imager, (b) Schematic of the imager and software workflow.

As shown in Fig. 1, our prototype is composed of the following components: a small foot-print 1" dual-RGB/NIR sensor module (2048×2048 pixel CMOSIS 4000 color RGB/NIR enhanced sensors, Ximea Gmbh, Germany), an electrically tunable lens (EL-16-40-TC), a 30 mW/cm^2 high-power 760 nm LED (below ANSI MPE guideline [10]), a 1 mW/cm^2 830 nm diode laser (under CLASS II laser safety level [11]), a 5" touch screen, and a GPU-embedded board (Jetson TX-2, Nvidia). The beam splitter/dichroic filter in the imager splits the light into RGB and NIR images (Fig. 1b). Furthermore, the on-board software processes and performs the dual image display onto a 4k Ultra High-Definition Screen intraoperatively. Mode 1 in this system permits a label-free, non-invasive localization of PTGs using NIRAF and mode 2 enables continuous visualization of vasculature and viability assessment of the PTG tissue using real-time dye free angiography with an 830 nm laser source.

In this work, we adopted the real-time dye-free imaging angiography technique to non-invasively visualize the tissue and vascular perfusion with false colors corresponding to their relative blood flow rates. Our software applied Eq. (1) to relate the speckle contrast values by measuring the relative velocity of red blood cells. The decorrelation time of the speckle intensity fluctuation, τ_c, was assumed to be inversely proportional to blood flow velocity, v [12].

$$v \propto \frac{1}{\tau_c} \quad (1)$$

Two different kernels and digitally adjustable upper and lower thresholding limits for the false color display were used to discriminate different perfusion levels. For the real-time *in vivo* application, we utilized a 5×5 spatial window with an exposure time of 14 µs at 70 frames-per-second. Either a 5×5 or 7×7 spatial filtering window has been widely settled upon as a good medium between spatial resolution and accuracy of the estimated speckle contrast [13]. Additionally, our software allows us to temporally blend a user-defined number of flow maps together to increase the signal to noise ratio [14]. For our pilot clinical study, we applied a 5×5×8 spatiotemporal window for increased resolutions.

B. Bench-top Testing Setup for System Characterization

In a benchtop setting, as shown in Fig. 2, working-distance, field-of-view, spatial resolution, and fluorescence sensitivity to 10 pmol of ICG (peak emission at 820 nm similar to that of the PTGs at 822 nm) diluted in 100 µL sterile water drop in the color detector card were tested and characterized. A microfluidic phantom with channels ranging from 0.2 - 1.8 mm was used to validate the system performance of spatial resolutions and real-time differentiation of relative flow rates.

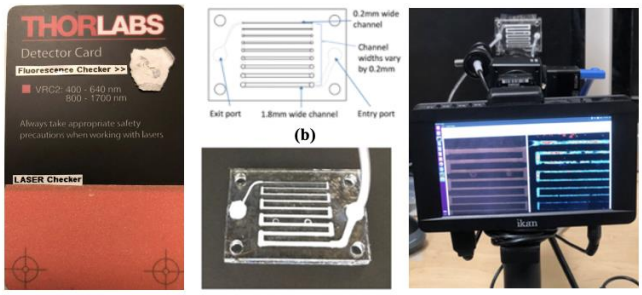

Figure 2. Images of an ICG detector card and a microfluidic phantom for the bench-top experimental setup. (a) ICG fluorescence testing with a detector card, (b) Microfluidic phantom schematic, channel widths range from 0.2 - 1.8 mm in increments of 0.2 mm, (c) Fabricated acrylic flow phantom infused with intralipid, and (d) *In vitro* phantom experimental setup with syringe pump with the prototype handheld device.

C. Clinical Study Protocol and Study Statistics

This pilot study's protocol was approved by the Kyungpook National University Chilgok Hospital Institutional Review Board (IRB FILE No. 2019-09-026-001). 10 patients who underwent lobectomy or total thyroidectomy were enrolled in our study. All surgeries were performed at a single institution by an experienced surgeon. For the initial feasibility study, the surgeon first exposed and identified PTGs with visual inspection, then allowed for imaging for 1 minute to confirm the NIRAF signals from the PTGs. An operator held the imager approximately 30 - 60 cm away from the surgical field. The total duration of the imaging time per each case was less than 5 minutes. Once the autofluorescence signals were confirmed from the exposed PTGs, perfusion assessment followed. After completion of the procedures, the PTG vascularity and perfusion were assessed again to confirm the PTG viability in the same manner. Due to the small number of patients involved in this pilot study, no formal power and sample size calculation were considered.

III. Results

A. ICG Fluorescence and Microfluidic Phantom Study

We performed the parameter calibration in the phantom studies shown in Fig. 3. Mode 1 clearly exhibits both color RGB and NIR fluorescence in the target ICG sample (Fig. 3a), while mode 2 shows detectable 0.2 - 1.8 mm channel widths at a working distance of 30 cm as well as the differentiation of relative flow rates in the microfluidic chamber.

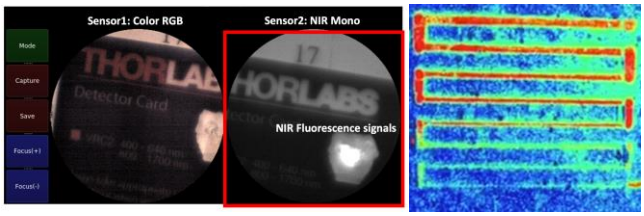

(a) **(b)**

Figure 3. Bench-top study results in (a) NIR fluorescence imaging mode highlighting ICG fluorescence and (b) NIR LSCI mode using a microfluidic phantom to differentiate different sized channels and relative flow rates.

B. Identification of PTGs using NIRAF

The autofluorescence signals emitted from the PTGs can be clearly noted in the NIR image without noticeable background noise signals (Fig. 4b). Frozen section results also confirmed that the autofluorescent tissues were indeed PTGs.

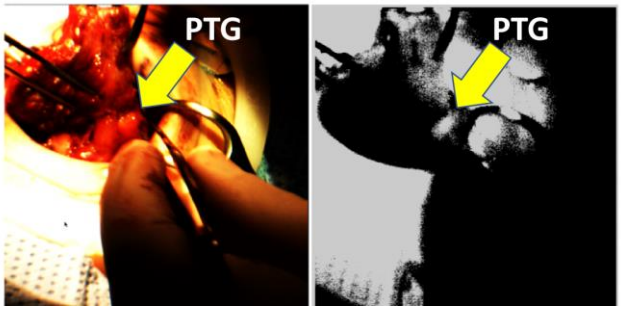

(a) **(b)**

Figure 4. PTG, indicated by the yellow arrows, visualized in (a) RGB image and (b) identified using NIRAF.

C. Viability Assessment using Dye-Free Angiography

The imager was switched to mode 2 and allowed for visualizing perfusion levels of PTGs. The blood flow in PTGs appeared red, which indicates high perfusion (Fig. 5b).

1) Viable PTG Cases

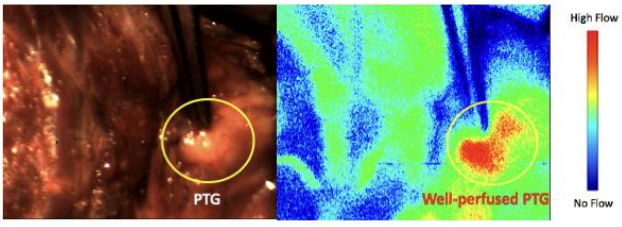

(a) **(b)**

Figure 5. Visualization of a healthy PTG in (a) RGB image and (b) intraoperative viability assessment using dye-free angiography. Color bar indicates relative blood flow rates. Note that the well-perfused PTG was shown in red when there are inflows with pulsation.

This was confirmed by the surgeon's assessment and further verified by patients' postoperative normal calcium (8.6 - 10.6 mg/dl) and PTH levels (10 - 65 pg/ml).

2) Non-viable PTG Cases

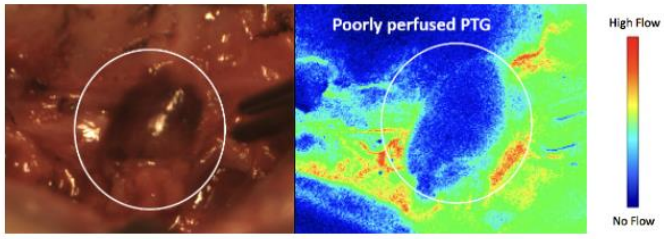

(a) **(b)**

Figure 6. Visualization of a non-healthy PTG in (a) RGB and (b) intraoperative viability assessment using dye-free angiography.

Non-viable PTGs were poorly perfused and appeared dark blue colored (Fig. 6). There was no venous drainage, and therefore the surgeon concluded that the PTG had no perfusion. Non-viable PTGs were autotransplanted in the sternocleidomastoid muscle.

3) Seemingly Normal but Non-viable PTG Cases

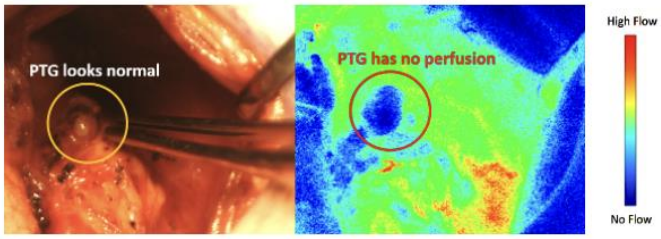

(a) **(b)**

Figure 7. Visualization of a seemingly healthy PTG in (a) RGB image and (b) intraoperative viability assessment using dye-free angiography showing a non-viable PTG.

4) Blood Vessels leading to PTG

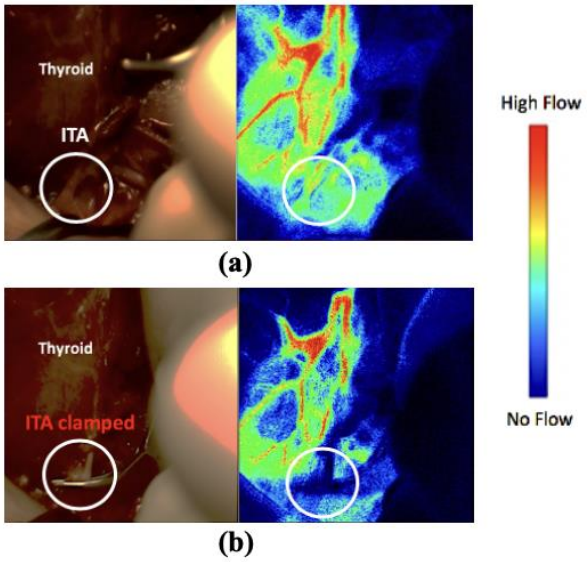

Figure 8. Visualization of blood flow through the inferior thyroid artery (a) before clamping and (b) after clamping using the dye-free angiography.

In the third case, the surgeon initially judged the PTG as a normal, healthy PTG because no discoloration or edema was

observed. However, little to no perfusion was found when evaluated by dye-free imaging angiography in mode 2 (Fig. 7b). After further dissection, the surgeon found that the feeding artery to the PTG was injured and confirmed that the PTG was non-viable. This indicates that perfusion assessments based on color or shape change of PTGs might not be effective. This PTG was also autotransplanted.

Finally, in addition to visualizing PTG perfusion, blood flow in the vessels leading to the PTGs were also observed in the superior and inferior thyroid artery (STA, ITA). As depicted in Fig. 8, the blood vessels were highlighted in red, showing high blood perfusion and flow rates. However, when the ITA was clamped, the blood flow was reduced and the clamped vessels appeared dark blue, indicating low perfusion and flow rates (Fig. 8b).

IV. Discussion

Early localization of PTGs during thyroid surgery is important for the preservation of its function and vascularity. ICG angiography has been studied to localize and assess vascularity of PTGs; however, there are still limitations to this approach because of its transient and qualitative assessment [8, 9].

In a recent study, Mannoh et al. quantitatively analyzed well- and poorly-vascularized PTGs using the LSCI technique with 91.5% accuracy [15], although the surgical light had to be turned off and the study was performed in a quasi-real-time manner during data acquisition. Moreover, processing took several minutes to display quantitative perfusion results. In comparison, our portable dye-free angiography device allows us to monitor tissue perfusion continuously in real-time, without interfering the surgical workflow. The OR light, surgical light, and head lamps do not need to be turned off. Specifically, our preliminary results suggested that the imager could evaluate real-time perfusion in three cases: a viable PTG, a non-viable PTG, and a seemingly viable but non-viable PTG. Most notably, the imager was able to detect vascular perfusion leading to PTGs without dye-injection, while other groups either used a temporally-limited ICG injection or were not able to confirm the vascularity near PTGs with the LSCI technique [15]. Another advantage is that our device can be iteratively used during surgery to determine the disruption of blood flow due to a transient vasoconstriction of PTGs.

In future studies, the performance of the imager will be improved upon our current spatial resolution (40 microns) to allow for clear visualization of refined details in tissues, micro-vessels, and pedicles feeding into the PTGs. Moreover, motion artifacts from the operator need to be addressed by incorporating our techniques in robust surgical arms or goggles. In addition, we plan to integrate a software that uses machine learning to increase accuracy and further assess perfusion levels quantitatively with statistical validation.

V. Conclusion

In this study, we demonstrated the early feasibility of a portable device that allows an instant shift between NIR fluorescence imaging and dye-free angiography. Our imager has the potential to be a practical tool for intraoperative identification and viability assessment of PTGs.

Acknowledgment

The authors would like to thank Dr. Gyeong Woo Cheon for his consultation on the technical developments and nursing staff at Kyungpook National University Chilgok Hospital for the clinical data collection.

References

[1] E. Karadeniz and M. N. Akcay, "Risk Factors of Incidental Parathyroidectomy and its Relationship with Hypocalcemia after Thyroidectomy: A Retrospective Study," *Cureus,* vol. 11, no. 10, p. e5920, Oct 16 2019, doi: 10.7759/cureus.5920.

[2] O. Edafe, R. Antakia, N. Laskar, L. Uttley, and S. P. Balasubramanian, "Systematic review and meta-analysis of predictors of post-thyroidectomy hypocalcaemia," *Br J Surg,* vol. 101, no. 4, pp. 307-20, Mar 2014, doi: 10.1002/bjs.9384.

[3] E. A. Mittendorf and C. R. McHenry, "Complications and sequelae of thyroidectomy and an analysis of surgeon experience and outcome," *Surg Technol Int,* vol. 12, pp. 152-7, 2004. [Online]. Available: https://www.ncbi.nlm.nih.gov/pubmed/15455320.

[4] C. Paras, M. Keller, L. White, J. Phay, and A. Mahadevan-Jansen, "Near-infrared autofluorescence for the detection of parathyroid glands," *J Biomed Opt,* vol. 16, no. 6, p. 067012, Jun 2011, doi: 10.1117/1.3583571.

[5] M. A. McWade *et al.*, "Label-free intraoperative parathyroid localization with near-infrared autofluorescence imaging," *J Clin Endocrinol Metab,* vol. 99, no. 12, pp. 4574-80, Dec 2014, doi: 10.1210/jc.2014-2503.

[6] Y. Shinden *et al.*, "Intraoperative Identification of the Parathyroid Gland with a Fluorescence Detection System," *World J Surg,* vol. 41, no. 6, pp. 1506-1512, Jun 2017, doi: 10.1007/s00268-017-3903-0.

[7] Y. J. Suh *et al.*, "Indocyanine green as a near-infrared fluorescent agent for identifying parathyroid glands during thyroid surgery in dogs," *Surg Endosc,* vol. 29, no. 9, pp. 2811-7, Sep 2015, doi: 10.1007/s00464-014-3971-2.

[8] J. Vidal Fortuny, V. Belfontali, S. M. Sadowski, W. Karenovics, S. Guigard, and F. Triponez, "Parathyroid gland angiography with indocyanine green fluorescence to predict parathyroid function after thyroid surgery," *Br J Surg,* vol. 103, no. 5, pp. 537-43, Apr 2016, doi: 10.1002/bjs.10101.

[9] N. M. Fanaropoulou, A. Chorti, M. Markakis, M. Papaioannou, A. Michalopoulos, and T. Papavramidis, "The use of Indocyanine green in endocrine surgery of the neck: A systematic review," *Medicine (Baltimore),* vol. 98, no. 10, p. e14765, Mar 2019, doi: 10.1097/MD.0000000000014765.

[10] R. J. Thomas, B. A. Rockwell, W. J. Marshall, R. C. Aldrich, S. A. Zimmerman, and R. J. R. Jr., "A procedure for multiple-pulse maximum permissible exposure determination under the Z136.1-2000 American National Standard for Safe Use of Lasers," *Journal of Laser Applications,* vol. 13, no. 4, pp. 134-140, 2001, doi: 10.2351/1.1386796.

[11] A. B. Parthasarathy, E. L. Weber, L. M. Richards, D. J. Fox, and A. K. Dunn, "Laser speckle contrast imaging of cerebral blood flow in humans during neurosurgery: a pilot clinical study," *J Biomed Opt,* vol. 15, no. 6, p. 066030, Nov-Dec 2010, doi: 10.1117/1.3526368.

[12] D. A. Boas and A. K. Dunn, "Laser speckle contrast imaging in biomedical optics," *J Biomed Opt,* vol. 15, no. 1, p. 011109, Jan-Feb 2010, doi: 10.1117/1.3285504.

[13] D. Briers *et al.*, "Laser speckle contrast imaging: theoretical and practical limitations," *J Biomed Opt,* vol. 18, no. 6, p. 066018, Jun 2013, doi: 10.1117/1.JBO.18.6.066018.

[14] J. Qiu, P. Li, W. Luo, J. Wang, H. Zhang, and Q. Luo, "Spatiotemporal laser speckle contrast analysis for blood flow imaging with maximized speckle contrast," *J Biomed Opt,* vol. 15, no. 1, p. 016003, Jan-Feb 2010, doi: 10.1117/1.3290804.

[15] E. A. Mannoh, G. Thomas, C. C. Solorzano, and A. Mahadevan-Jansen, "Intraoperative Assessment of Parathyroid Viability using Laser Speckle Contrast Imaging," *Sci Rep,* vol. 7, no. 1, p. 14798, Nov 1 2017, doi: 10.1038/s41598-017-14941-5.